Plasma Medicine, 2(1-3): 1–18 (2012)

Active Species Concentrations in Pure N_2 and Ar/x%N_2 Flowing Late Afterglows at Reduced Pressure: Implications for the Sterilization of the Medical Instrumentation

Hayat Zerrouki[1,2], Laure Barreyre[1,2], Gérald Ledru[1,2], Sarah Cousty[3], André Ricard[1,2] and Jean-Philippe Sarrette[1,2]*

[1]Université de Toulouse; UPS, INPT; LAPLACE (Laboratoire Plasma et Conversion d'Energie), Bât. 3R2, 118 route de Narbonne, F-31062 Toulouse cedex 9, France; [2]CNRS, LAPLACE, F-31062 Toulouse, France; [3]Université de Toulouse, UPS, Laboratoire Parodontites et Maladies Générales, Faculté de Chirurgie Dentaire de Toulouse, 3 Chemin des Maraîchers, 31062 Toulouse cedex 9, France

*Address correspondence to: Jean-Philippe Sarrette, LAPLACE, Université Paul Sabatier, Bât. 3R2, 118 route de Narbonne, F-31062 Toulouse cedex 9, France ; Tel.: 33 (0)5 61 55 68 98; Fax: 33 (0)5 61 55 63 32; Email : jean-philippe.sarrette@laplace.univ-tlse.fr

ABSTRACT: The present paper is devoted to the characterization of the late afterglow region of N_2 and Ar–N_2 flowing discharges. Optical emission spectroscopy is used to quantify the concentrations of the chemical species able to interact with microorganisms in the treatment chamber. Herein, we show that the production of nitrogen atoms in the afterglow of a reduced-pressure flowing microwave discharge can be increased using Ar–N_2 mixtures instead of pure nitrogen. At 45 cm from the discharge, the maximum concentration of atoms, obtained for the Ar–15%N_2 mixture, is 2.2×10^{21} m^{-3} at 9 Torr with an injected microwave power P_{MW} of 100 W and 2.9×10^{21} m^{-3} at 200 W. Compared with the maximum N atom concentrations obtained in pure nitrogen at 4 Torr, this result corresponds to an increase of 120% at 100 W and 45% at 200 W.

We have verified that these results can be obtained while conserving full late afterglow conditions at a temperature equal to the room temperature at 100 W and not exceeding 35°C at 200 W. Under such conditions, the concentrations of the NO(A and B) excited states, formed from the impurities of the flowing gas, are low. For pure nitrogen, the concentration of the N_2(A) metastable state was also measured at the end of the pink afterglow, where it is assumed to be maximal; it was 2.5×10^{16} m^{-3}.

Nitrogen atoms are the major reactive species in the late afterglow region. They are believed to be responsible for the antibacterial properties of pure N_2 and Ar–N_2 flowing afterglows. To verify this assumption, the Ar–15%N_2 flowing afterglow was applied to inactivate *Escherichia coli* bacteria, and the results were compared with previous studies performed in pure nitrogen and using the same microbiological protocol. With 40 min of exposure to Ar–15%N_2 afterglow ([N] = 2.9 10^{21} m^{-3}) at 32°C, a 6 log decrease of the initial bacteria population was obtained, while the same 6 log reduction could only be reached at 60°C with pure nitrogen afterglow ([N] = 1.0×10^{21} m^{-3}).

KEY WORDS: Afterglow plasma processes, nitrogen, optical emission spectroscopy, sterilization, metastable states

I. INTRODUCTION

Today, the autoclave is the most widely used method for the sterilization of reusable medical instruments. It is efficient for the sterilization of packaged instruments that may present complex shapes, and it is also inexpensive, relatively fast (~1 h), easy to use, and free of toxic byproducts. However, the maximum temperature reached during the autoclaving cycle is of 134°C, and it can only be used on instruments that can withstand this temperature without damage. For heat-sensitive instruments, the alternative sterilization gaseous reagents, the most common being ethylene oxide (EtO). But EtO is a very toxic gas that requires great caution in its handling and use. In the presence of residual water, EtO is transformed in ethylene glycol, which is an inefficient biocidal. EtO also reacts with the chlorine atoms of PVC materials to produce chloroethanol, another toxic gas for which the sterilized devices must be ventilated after sterilization, sometimes for as long as 24 hours.

During the last 15 years, different gas discharges operating at pressures ranging from low pressure (≈0.1 Torr)[1] to atmospheric pressure[2] have been studied to develop a plasma sterilizer that will treat instruments either inside the discharge (i.e., direct treatment) or submitted to the discharge effluents (i.e., remote treatment) in the afterglow region.

Due to the presence of large concentrations of energetic (electrons, ions) and reactive species (radicals, atoms, excited states able to emit UV radiation), direct treatments generally produce the rapid death of the exposed microorganisms and achieve a sterile state (i.e., a 6 log reduction of the initial bacterial concentration) in some tens of seconds.[3,4]

Remote treatments require longer times to reach the same sterile state, but they provide the advantage of an homogeneous treatment in large-volume reactors (up to many liters), which allows better diffusion of the active species.[5,6]

In one of our previous works, we showed that the antimicrobial efficiency of a pure nitrogen flowing afterglow can be largely improved by an increase of the concentration of the nitrogen atoms present in the treatment chamber.[7]

In pure nitrogen discharges, the electron energy distribution function (EEDF) is depleted above 3 eV because of the low mean vibrational excitation of the $N_2(X)$ molecules. This is not the case for argon discharges for which the EEDF extends to higher energies, due to the presence of the first excitation threshold at 11.5 eV. Consequently, the addition of small percentages of nitrogen to the argon carrier gas may improve the nitrogen dissociation through two main channels: (1) direct electron impact dissociation in the discharge by more energetic electrons, and (2) collisions between argon metastable molecules and nitrogen molecules in the afterglow.[8]

In the present paper, Ar–x%N_2 (x < 20%) afterglows are characterized, with a particular focus on N atom production and the application of these afterglows to the eradication of microorganisms.

The paper is organized in three main parts: section II describes the experimental arrangement and the microbiological protocol. Section III concerns the optimization of

the atomic nitrogen production in Ar–x%N_2 mixtures. Pure N_2 and Ar–x%N_2-flowing afterglows were investigated in this study and are presented in terms of gas temperature and of absolute concentrations of the chemical species of interest (N atoms, $N_2(A)$ metastable states, and NO radiative states). Finally, in part IV our evaluation of the antimicrobial efficiency of the optimal Ar/N_2 mixture is presented and compared with that of the pure N_2 afterglow.

II. EXPERIMENTAL ARRANGEMENT AND MICROBIOLOGICAL PROTOCOL

A. Reduced-Pressure Flowing Afterglow Setup

In this setup, the gas flow is generated by a continuous injection of nitrogen and argon (Linde, 99.995% purity), monitored by Brooks 5850TR mass flow meters, and pumped by a primary vacuum rotary vane pump (Edwards E2M28). It is excited by a Sairem GMP 03 KE/D microwave generator connected to a surfatron cavity and operating at 2.45 GHz, with an output power P_{MW} adjustable between 0 and 300 W. The discharge is sustained in a quartz tube 5 mm in internal diameter (i.d.), extended by a bent quartz tube of 17 mm i.d. and connected to a 4.5-L Pyrex reactor (15 cm i.d. and 25 cm height). The bend prevents the UV radiation coming from the discharge to reach the bacteria exposed in the treatment chamber (Fig. 1). The distance d between the surfatron cavity and the bent tube can be modified between 5 and 25 cm; the length of the bent quartz tube is fixed at 40 cm. During the NO titration, an additional Ar-2%NO injection is used, connected to the 17 mm i.d. tube. The gas pressure is measured in the treatment chamber by a MKS Baratron capacitive transducer located on the top of the chamber and is regulated with a throttle valve placed downstream.

The spectral emission of the afterglow is collected by an optical fiber that can be moved along the injection tubes and along the reactor and proceeds to the entrance slit of an Acton Spectra Pro 2500i spectrometer (focal length of 50 cm, mounted with three gratings: 1200, 2400, and 3600 gr mm^{-1}), equipped with a Pixis 256E CCD detector (front illuminated 1024 × 256 pixels).

B. Microbiological Protocol

The *E. coli* strain (CIP: 54.8 T) provided by the International Collection of Pasteur was used in this method to facilitate the comparison of these results with our previous results, which were obtained in pure nitrogen with the same microbiological protocol.[7]

Before exposure, a broth containing an average bacteria concentration of 10^8 ml^{-1} is prepared. A 10-µl droplet of this broth is deposited on a sterile glass sheet, placed in the treatment chamber, and slowly desiccated by vacuum exposure (10 min at 0.01 Torr), resulting in a bacterial film of 5–10 mm in diameter which is exposed to the afterglow.

After exposure, the glass sheet and the bacterial film containing living and nonliving bacteria are immersed in 1 ml of LB broth. Bacteria are then retrieved using a 90-s gentle mechanical agitation. A total of 100 µl of the recovery suspension is retrieved, eventu-

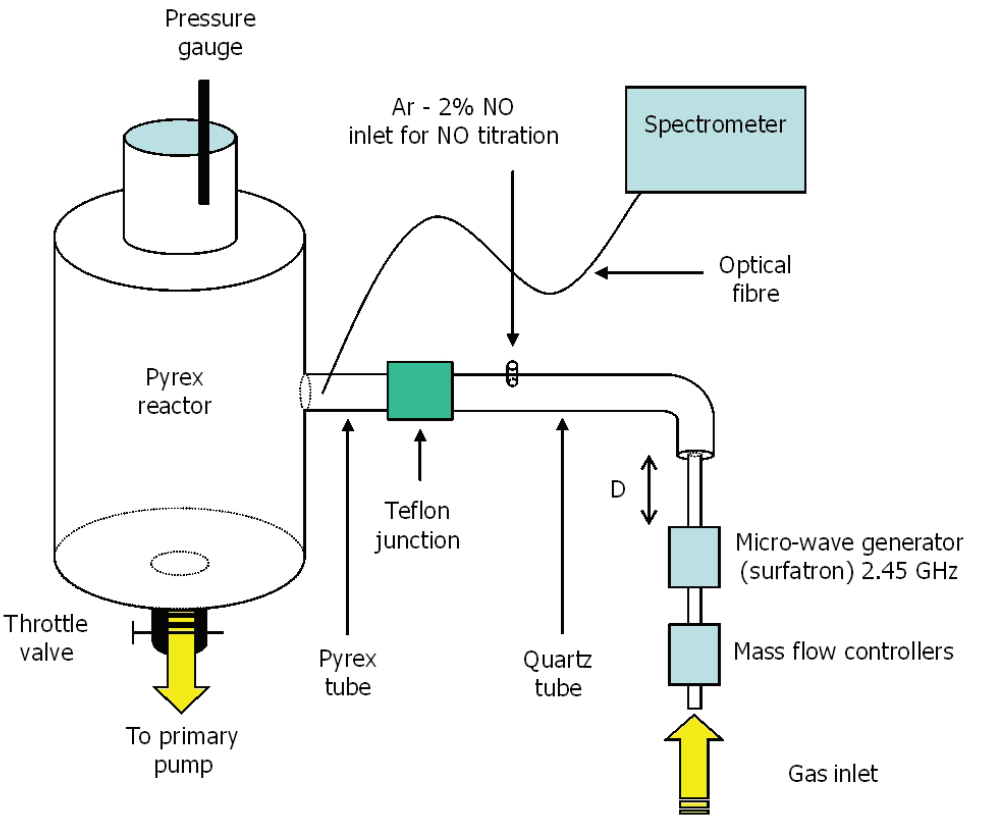

FIG. 1: Experimental setup of the reduced pressure flowing microwave afterglow.

ally diluted, and spread on agar in Petri dishes. The colonies formed from the surviving bacteria counted after 24 h of incubation at 37°C. The sterile level is considered to have been reached when no colonies are observed and when the recovery suspension shows no turbidity after an overnight incubation. Each experiment was repeated three times.

III. AFTERGLOW DIAGNOSTICS

A. Nitrogen Concentration

1. Pure Nitrogen

In the pink afterglow, the population of the $N_2(B)$ state responsible for the first positive (1+) emission is essentially due to the collisions between vibrationally excited ground-state molecules with the $N_2(A)$ metastable state:

$$N_2(A) + N_2(X, 5 \leq v \leq 14) \rightarrow N_2(B, v') + N_2(X, v=0), \quad (1)$$

while in the late afterglow, only the $N_2(B, v'=11)$ state remains substantially populated by the three-body recombination of the nitrogen atoms:

$$N + N + N_2 \rightarrow N_2(B, v'=11) + N_2, \quad (2)$$

producing an apparent intensification of the 1+ emission around 580 nm:

$$N_2(B, v'=11) \rightarrow N_2(A, v''=7) + h\nu\ (580\ nm). \quad (3)$$

As a consequence, depending on the afterglow operating conditions and at a given distance from the discharge, only a fraction k_L of the intensity measured at 580 nm is due to the atomic recombination, and the changes observed in the vibrational intensity distribution of the 1+ emission (Fig. 2) can then be used to monitor the relative N atom concentration during the transport between the discharge and the late afterglow region. For gas pressure higher than 1 Torr, the 1+ intensity at 580 nm I_{580nm} is then related to the N atom concentration by the following formulas:

$$k_L I_{580\,nm} \propto \left[N_2(B, v'=11)\right] \propto \left[N\right]^2 \quad (4)$$

$$\left[N\right] = K_{norm}\sqrt{k_L I_{580nm}} \quad (5)$$

As proposed by Bockel et al.,[9,10] the k_L coefficient can be obtained by directly comparing the measured relative vibrational intensity distributions $R_{B,v'}$ of the $v' = 7–12$ bands of the $\Delta v = –4$ sequence of the 1+ system and the theoretical $R_{B,v'}$ distributions calculated for the full pink afterglow ($k_L = 0$), for the full late afterglow ($k_L = 1$), or for intermediate cases ($0 < k_L < 1$):

$$R_{B,v'} = \frac{I\left[N_2(B, v')\right]}{\sum_{v'=7}^{v'=12} I\left[N_2(B, v')\right]} \quad (6)$$

The classical NO titration method can then be used to obtain the normalization constant K_{norm} and the absolute concentrations of the nitrogen atoms.[10] The proportionality law established in Eq. (5) between the square root of the I_{580nm} emission measured in full late afterglow conditions ($k_L = 1$) and the N-atom absolute concentration given by NO titration was verified as shown in Fig. 3. The variations of the N-atom concentration measured for a N_2 flow rate of 1.0 slpm at the center of the treatment reactor for different pressures and different injected microwave powers P_{MW} are shown in Fig. 4.

2. *Ar–x%N_2 mixtures (x < 20%)*

In the presence of argon, the relative vibrational intensity distribution of the $\Delta v = –4$ sequence of the 1+ emission is modified, as shown in Fig. 5. For high N_2 percentages ($10\% < x < 20\%$), an increase in the emission of the 10-6 and 9-5 bands of the sequence,

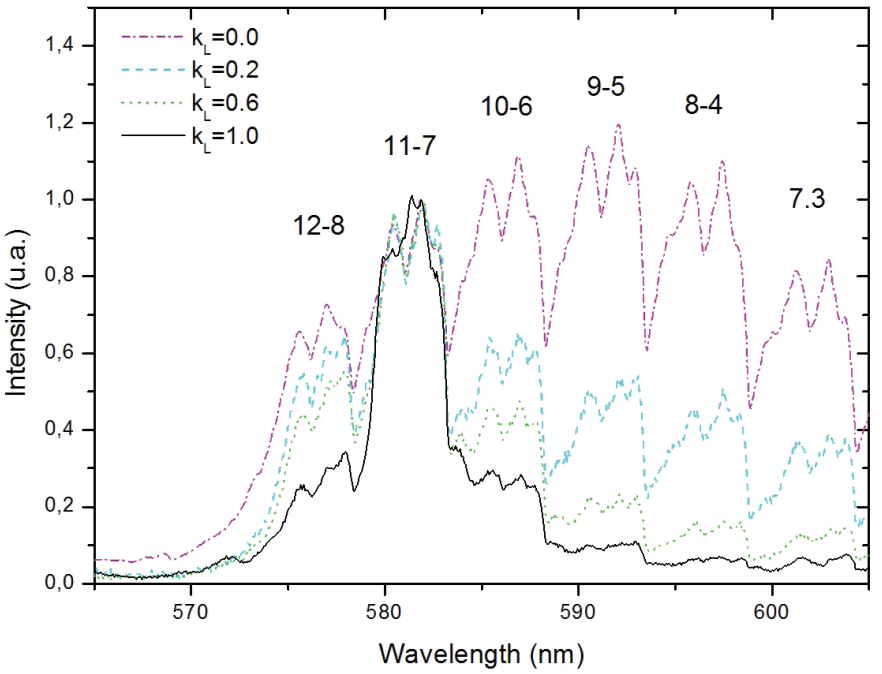

FIG. 2: Normalized emission spectra of the Δv = –4 sequence of the first positive system of N_2 measured in pure nitrogen for different afterglow conditions. The k_L parameter represents the fraction of the first positive intensity at 581 nm due to the three-body recombination of the nitrogen atoms through reactions (2) and (3).

compared with the 11-7 band can be observed. For low N_2 percentages (x < 5%), the emission of the 8-4 band is favored. These modifications can be attributed to the presence of metastable states of argon (Ar^m, $E^m > 11.55$ eV) in the afterglow; their energy is enough to enhance the production of the $N_2(C)$ state by a selective excitation transfer,[11]

$$Ar^m(^3P_0, {}^3P_2) + N_2(X) \rightarrow Ar + N_2(C), \quad (7)$$

and this transfer is followed by a radiative de-excitation toward the $N_2(B)$ and $N_2(A)$ states:

$$N_2(C) \rightarrow N_2(B) + h\nu \text{ (nitrogen second positive system, 2+)} \quad (8)$$

$$N_2(B) \rightarrow N_2(A) + h\nu \text{ (nitrogen first positive system, 1+).} \quad (9)$$

As long as the dominant process for the population of the $N_2(B,v' = 11)$ state remains the atomic three-body recombination [reaction (2)], the pure N_2 method remains valid to obtain the N-atom concentration in the Ar–x%N_2 afterglows at the condition under which the k_L coefficient from the theoretical vibrational intensity distributions $R_{B,v'}$ calculated

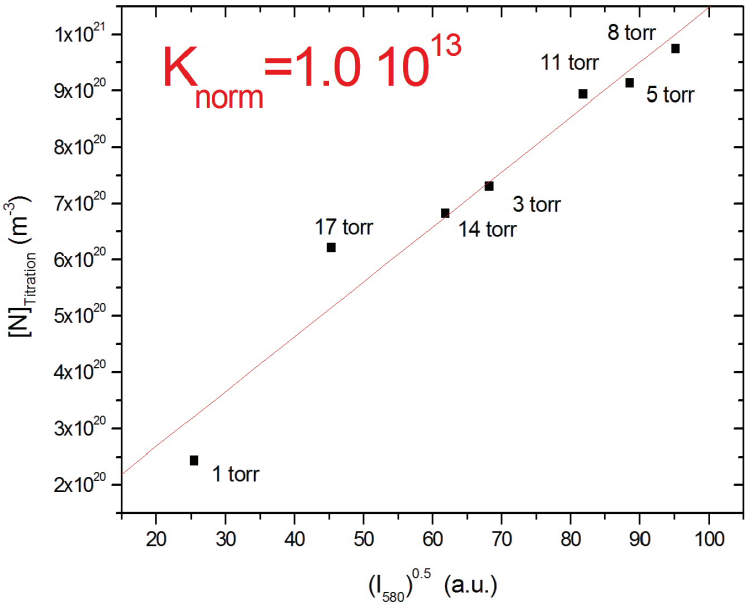

FIG. 3: Variation of the N-atom absolute concentration given by NO titration with the square root of the I_{580nm} emission measured for different pressures at the reactor entrance in full late afterglow conditions (k_L = 1). The proportionality between the two quantities gives the normalization constant of eq. (5).

for each mixture. The normalized vibrational intensity distributions of the theoretical $R_{B,v'}$ are given in Fig. 6a for the pure N_2 afterglow and in Fig. 6b for the Ar–15%N_2 afterglow. For the Ar–N_2 mixtures, the full pink afterglow condition (k_L = 0) was taken at the distance to the surfatron at which the intensity emitted by the first negative emission corresponding to the transition at 391.4 nm between the N_2^+ (B, v' = 0) and N_2^+ (X, v" = 0) states of the molecular ion) is maximal. The full late afterglow condition (k_L = 1) was considered to have been reached when the observed $R_{B,v'}$ relative distribution became independent from the distance to the surfatron.

The corresponding variations of the absolute N atom concentration measured at the reactor entrance with the pressure and the percentage of nitrogen in the mixture are shown in Fig. 7. The N-atom production increases rapidly for percentages of nitrogen less than 10% and shows a saturation for higher percentages between 3 and 15 Torr. Comparing the atomic concentrations measured in the reactor for pure nitrogen and for the Ar–15%N_2 mixture (Fig. 8) at constant power and pressure, the N atom density is always higher and obtained at a higher pressure in the mixture than in pure nitrogen. The increase of the N atom concentration in the two afterglows is 120% at 100 W and 45% at 200 W. There are also more atoms at 100 W and 9 Torr in the Ar–15%N_2 mixture than at 200 W and 5 Torr in pure nitrogen. Consequently, we chose to use the Ar-15%N_2 mixture for the microbiological tests analyzed in section IV.

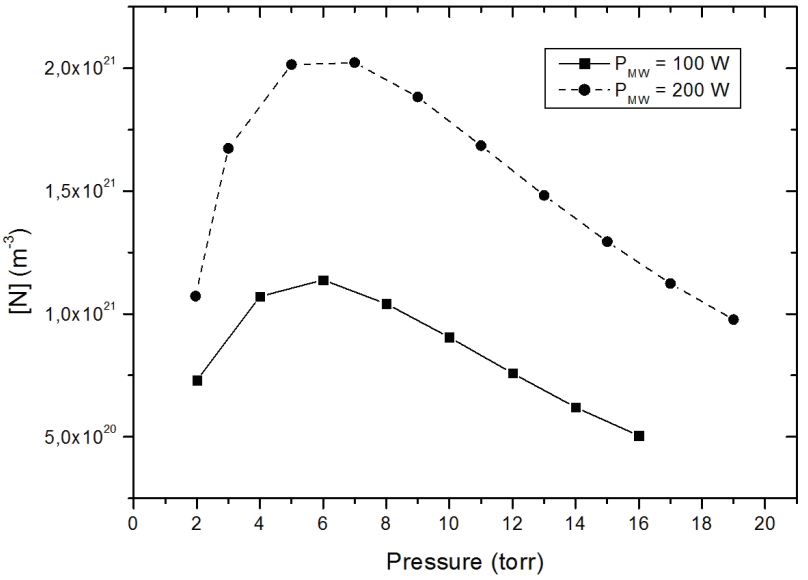

FIG. 4: Variation of the N-atom absolute concentration measured in pure N_2 in the treatment reactor (Q_{N2} = 1.0 slpm, d = 5 cm).

Notably, for the typical operating conditions of the afterglows used in this study ($p \geq 2$ Torr, Qcarrier = 1.0 slpm, $P_{MW} \leq 200$ W and $x \leq 20\%$), full late afterglow conditions were reached for $d > 5$ cm, corresponding to a total distance of 45 cm between the surfatron and the treatment chamber. This distance was used for all the microbiological exposures.

B. $N_2(A)$ Concentration

Due to its long radiative lifetime (≈ 2 s) and its high potential energy (6.17 eV), the first metastable state $N_2(A)$ of the nitrogen molecule may have a significant impact on the chemistry of nitrogen-containing afterglows and their antimicrobial activity. The methods used to measure the $N_2(A)$ absolute concentration were generally based either on the emission of the forbidden Vegard-Kaplan system $N_2(A^3\sigma_u^+ \rightarrow X\,^1\sigma_g^+)$ around 300 nm[12,13] or on absorption techniques.[14,15] In the first case, the uncertainty is high due to the low intensity of the band emission, having an absolute transition probability of 0.16 s^{-1} for the most intense 0-6 band.[16] In the latter case, the reliability of the measurement remains poor for metastable densities around 1016 m^{-3}, as expected in the nitrogen afterglow.[15,17]

$$NO + N \rightarrow O + N_2 \quad (10)$$

$$N + O + N_2 \rightarrow NO(B, v'=0) + N_2 \quad (11)$$

$$NO(B, v=0) \rightarrow NO(X, v''=8) + h\nu_{320nm} \quad (12)$$

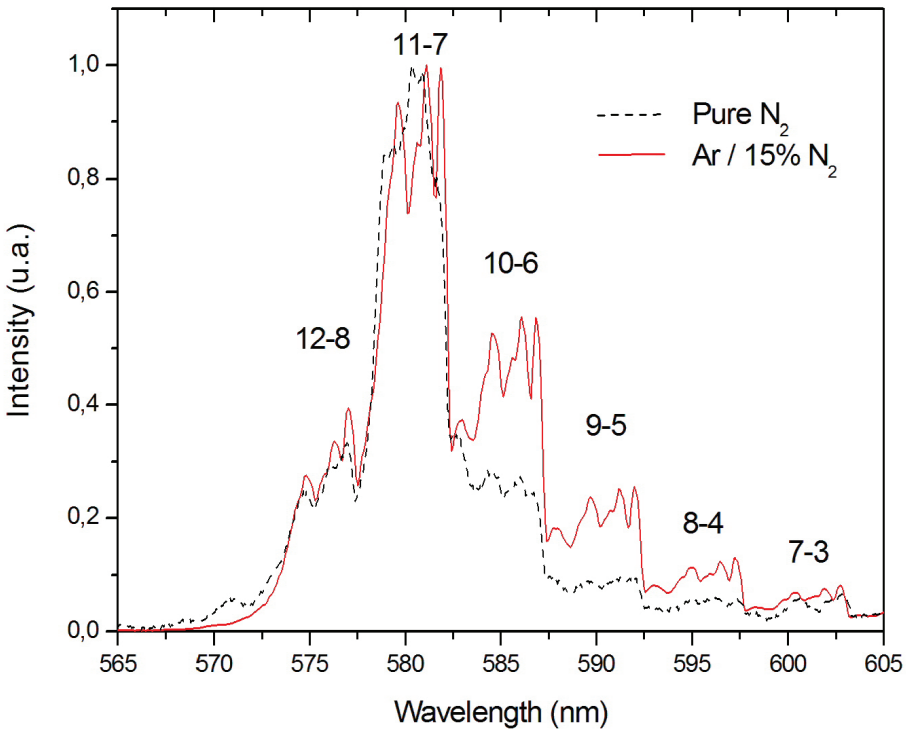

FIG. 5: Comparison between the vibrational intensity distribution of the Δv=–4 sequence of the first positive system of N_2 measured in full late afterglow conditions in pure nitrogen and in the Ar–15% N_2 mixture ($Q_{carrier}$ = 1.0 slpm, p = 5 Torr, P_{MW} = 100 W).

and

$$NO + N_2(A) \rightarrow NO(A, v'=0) + N_2 \quad (13)$$

$$NO(A, v'=0) \rightarrow NO(X, v''=2) + h\nu_{248nm} \quad (14)$$

The intensities emitted by the two bands are related to the concentrations of the emitting states according to two formulas:

$$I_{246nm} = \left[NO(A, v'=0)\right] A_{\gamma}^{0-2}\, bG(248nm)/248nm \quad (15)$$

$$I_{320nm} = \left[NO(B, v'=0)\right] A_{\beta}^{0-8}\, bG(320nm)/320nm \quad (16)$$

where A_{γ}^{0-2} and A_{β}^{0-8} are the vibrational transition probabilities of the two bands, $G(\lambda)/\lambda$ is the relative spectral function of the optical system used for the acquisition, and b is a geometrical multiplicative constant, independent of wavelength.

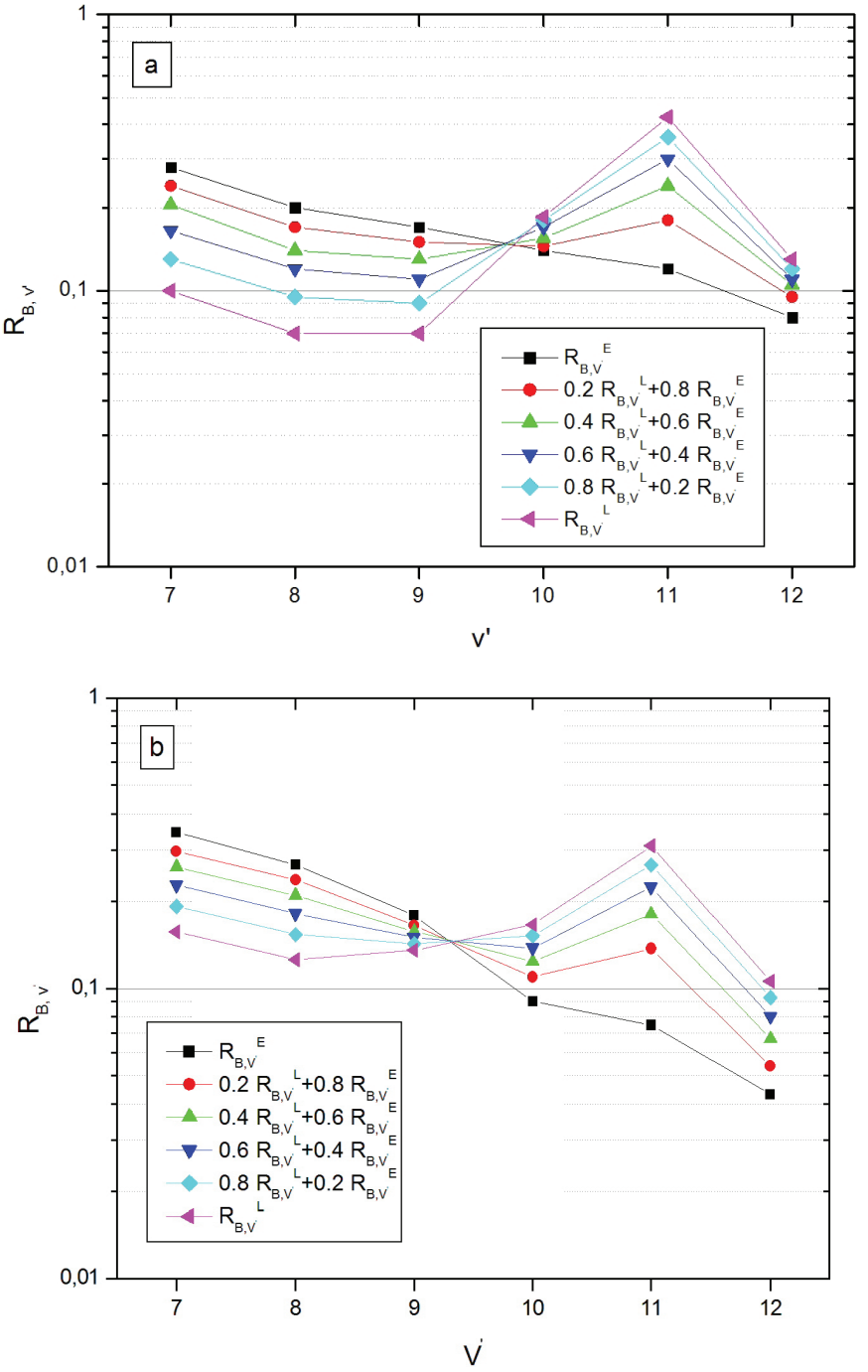

FIG. 6: Normalized vibrational intensity distributions $R_{B,v'}$ calculated for (a) pure nitrogen (taken from [9]) and (b) the Ar–15%N_2 mixture (this work). $R_{B,v'}^{E}$ corresponds to a full early afterglow distribution and $R_{B,v'}^{L}$ corresponds to a full late afterglow distribution.

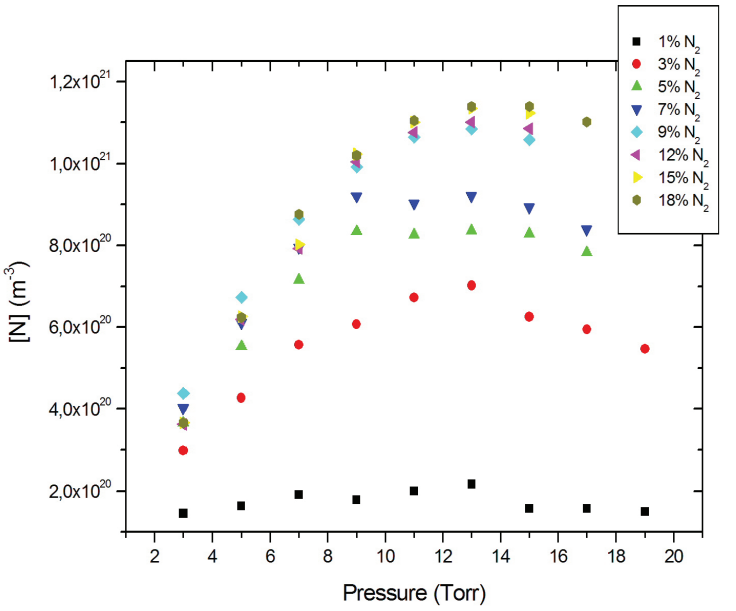

FIG. 7: Variation of the N-atom absolute concentrations measured at the reactor entrance with the N_2 percentage of the Ar–N_2 mixture. (Q_{Ar} = 1.0 slpm, P_{MW} = 100 W, d = 5 cm).

Using the quasi-stationary approximation and the main kinetic mechanisms for the creation and the destruction of the emitting states given in Table 1 with their corresponding rate coefficients A_i and k_i, it follows that

$$\left[NO(A,v'=0)\right] = \frac{k_1}{A_1 + k_2\left[N_2\right]} \left[N_2(A)\right] \left[NO\right] \tag{17}$$

$$\left[NO(B,v'=0)\right] = \frac{k_3\left[N_2\right]}{A_2 + k_4\left[N_2\right]} \left[N\right] \left[O\right] \tag{18}$$

The intensity ratio between the two bands is then equal to

$$\frac{I_{248nm}}{I_{320nm}} = \frac{Q_1}{Q_2} \frac{\left[NO\right]}{\left[O\right]} \frac{\left[N_2(A)\right]}{\left[N\right]} \tag{19}$$

with

$$Q_1 = \frac{k_1}{A_1 + k_2\left[N_2\right]} A_\gamma^{0-2} \frac{G(248nm)}{248nm} \tag{20}$$

$$Q_2 = \frac{k_3\left[N_2\right]}{A_2 + k_4\left[N_2\right]} A_\beta^{0-8} \frac{G(320nm)}{320nm} \tag{21}$$

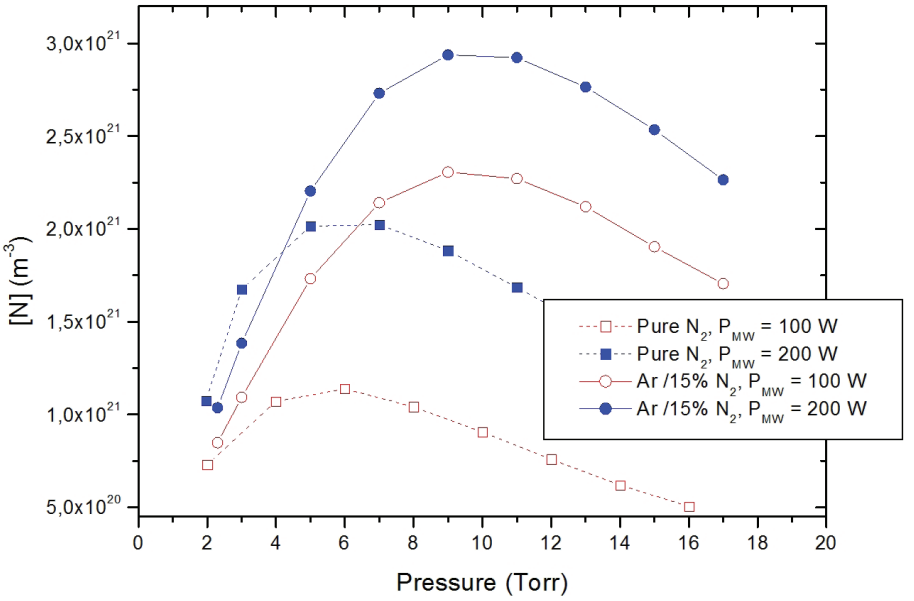

FIG. 8: Comparison between the N-atom absolute concentrations measured in the treatment reactor in pure N_2 and in the Ar–15%N_2 mixture. ($Q_{carrier}$ = 1.0 slpm, d = 5 cm).

TABLE 1. Main creation and loss mechanisms involved in the chemistry of the NO(A,v ' = 0) and NO(B,v ' = 0) radiative states. The given rate coefficients are taken from Pointu et al.[18]

Observed emissions	Creation mechanisms	Loss mechanisms
	$NO + N_2(A) \rightarrow NO(A, v'=0)$	$NO(A, v'=0) + N_2 \rightarrow products$
$NO(A,v'=0)$		
	$+ N_2$	$k_2 = 4.910^{-14}\ cm^3s^{-1}$
$\rightarrow NO(X,v''=2) + h\,\Delta_{248nm}$		
	$k_1 = 6.610^{-11}\ cm^3s^{-1}$	$NO(A, v'=0) \rightarrow NO(X) + hv$
$A_\gamma^{0-8} = 1.12410^6\ s^{-1}$		
		$A_1 = 4.910^6\ s^{-1}$
	$N + O + N_2 \rightarrow NO(B, v'=0)$	$NO(B, v'=0) + N_2 \rightarrow products$
$NO(B,v'=0)$		
	$+ N_2$	$k_4 = 6.110^{-13}\ cm^3s^{-1}$
$\rightarrow NO(X,v''=8) + h\,\Delta_{320nm}$		
	$k_3 = 2.910^{-34}\ cm^6s^{-1}$	$NO(B, v'=0) \rightarrow NO(X) + hv$
$A_\beta^{0-8} = 8.51310^4\ s^{-1}$		
		$A_2 = 4.710^5\ s^{-1}$

As the main reaction channels for the O and NO species follow reaction (10), with a rate coefficient $k_{10} = 1.82\ 10^{-11}$ cm^3 s^{-1} [20], the three-body recombination reaction is

$$N + O + N_2 \rightarrow NO + N_2, \text{ with } k_{22} = 1.02\ 10^{-32} \text{ cm}^6 \text{ s}^{-1} \text{ [20]}. \quad (22)$$

The [NO]/[O] ratio can be approximated to (k_{22} [N_2])/k10), and the [N_2(A)] absolute concentration can be directly deduced from the measurement of the intensity ratio I_{246nm}/I_{320nm} and from the previously determined absolute N atom concentration (*see* section III.A. Nitrogen Concentration):

$$\left[N_2(A)\right] = 5.75\ \ 10^{-22}\left[N\right]\ \ \left[N_2\right]\ \ \frac{Q_1}{Q_2}\ \ \frac{I_{246nm}}{I_{320nm}} \quad (23)$$

The N_2(A) absolute concentrations measured using this method in the pure nitrogen afterglow at different distances from the surfatron are presented in Fig. 9. With these afterglow operating parameters, the measurement points correspond to an afterglow time between 7 and 18 ms, located in the transition zone between the end of the pink afterglow (where the metastable concentration is supposed to present a maximum) and the beginning of the late afterglow. The measured values are in good agreement with the concentrations measured by Sadeghi et al. using an intracavity laser absorption spectroscopy method[15] and with the values calculated by Levaton et al.[17] It was not possible to measure the N_2(A) concentration closer to the treatment reactor because of the weakness of the NOγ and NOβ emissions, but it is reasonable to think that it is low (less than

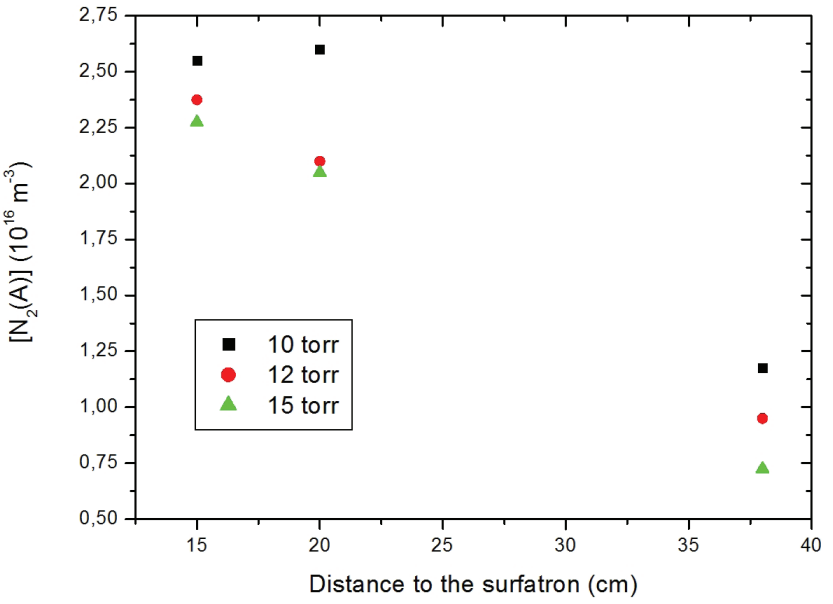

FIG. 9: Absolute concentration of the N_2(A) metastable measured in the pure nitrogen afterglow. (Q_{N2} = 0.5 slpm, P_{MW} = 100 W).

10^{15} m^{-3}, compared with the N atom concentration of 10^{21} m^{-3}). In such conditions, the $N_2(A)$ metastable state is not expected to play a major role in the death of microorganisms in the late nitrogen afterglow.

To our knowledge, the rate coefficients for the specific excitation and de-excitation of the radiative states NO(A, v' = 0) and NO(B, v' = 0) in the presence of argon are not available in the literature, and the corresponding Q_1 and Q_2 constants cannot be calculated in the Ar-N_2 mixtures. Nevertheless, the presence of the metastable states of Ar in the Ar-N_2 afterglows is expected to produce higher $N_2(A)$ concentrations than in pure N_2 through reaction (7) and the radiative cascades in reactions (8) and (9).

C. UV Emission

In the UV-C range (200–290 nm), the highest biocidal efficiency of most of the microorganisms is between 254 and 260 nm, corresponding with the maximum absorption of the DNA.[21,22] In N_2–O_2 afterglows at reduced pressure, this wavelength range is covered by the emission of the NOβ system (200–380 nm), in which production can be optimized (essentially through reaction (11)) to achieve sterilization in combination with chemical erosion by N and O atoms and heating. In flowing late afterglows, the maximum of the UV production is obtained for mixtures containing approximately 0.3% oxygen.[10,23]

In the pure nitrogen and Ar–N_2 afterglows studied here, oxygen was present as an impurity, and its concentration did not exceed 0.005%. With our exposure conditions ($p < 10$ Torr, $d > 5$ cm, $P_{MW} \leq 200$ W), the NO β system can be observed in the treatment chamber, with a very low intensity, hardly distinguishable from the background signal of the acquisition system. As a consequence, we do not believe that UV irradiation plays a major role in the sterilization process.

D. Gas Temperature

The gas temperature T_g of the afterglows at the entrance of the reactor (d = 15 cm) was estimated using optical emission spectroscopy through the relative variation of the emission of two sub-substructures of the 2-0 band of the 1+ system of N_2 around 775 nm. This method, described in detail by Britun et al.,[24] gives access to the rotational temperature, assumed here to be equal to Tg and also valid in pure nitrogen than in the Ar-N_2 mixtures. This method provides the advantage of very good sensitivity at low temperatures ($Tg < 400$ K), as the intensity ratio strongly varies in this temperature range.

The temperatures of the afterglows studied in this work are listed in Table 2. For the two gases, the temperature is equal to the room temperature for an injected microwave power of 100 W and increases by 5–10°C when PMW reaches 200 W.

IV. STERILIZATION RESULTS

With a pure nitrogen afterglow, Villeger et al. showed that it was possible to obtain a 2.5-log decrease of the initial *E. coli* population at room temperature (Fig. 10).[7] This result

TABLE 2. Gas temperatures of the afterglows measured using the P1/P2 spectral peaks ratio method presented in Britun et al. ($Q_{carrier}$ = 1.0 slpm, p = 5-10 Torr, d = 15 cm).

	P_{MW} = 100W	P_{MW} = 200W
Pure N_2	23°C	30°C
Ar - 15% N_2 mixture	25°C	32°C

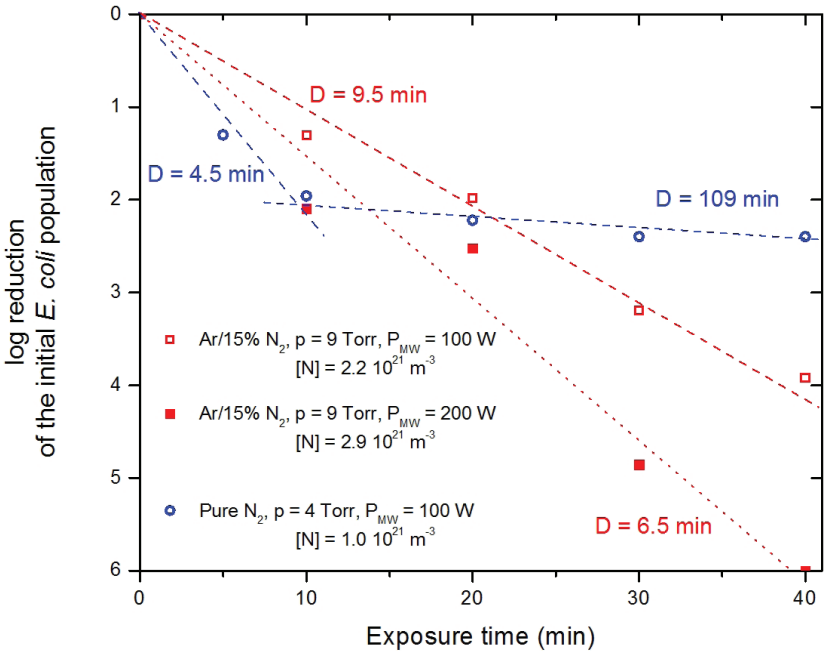

FIG. 10: Survival curves obtained for *E. coli* exposed to different late afterglows in the treatment chamber at temperatures close to the room temperature. (d = 5 cm, $Q_{carrier}$ = 1.0 slpm). Linear least-square fits are given, with the corresponding D values.

was obtained in 40 min of exposure with the same experimental setup used in the present work and the same microbiological protocol. The injected microwave power was set to 100 W, with a nitrogen flow rate of 1.0 slpm and an operating pressure fixed at 4 Torr to maximize the nitrogen atom concentration ([N] = 1.0×10^{21} m^{-3}) in the treatment chamber (Fig. 4). The survival curve obtained clearly shows two slopes. Cell death occurred rapidly during the first 10 minutes of exposure, with a D value (exposure time required to decrease a given population of bacteria by a factor of 10) close to 4.5 min. After the first 10 min of exposure, the antimicrobial efficiency decreased rapidly, with a D value of 109 min.

With the Ar–15%N_2 mixture, for the same injected microwave power of 100 W, the optimal N-atom concentration was [N] = 2.2×10^{21} m^{-3} at 9 Torr. A unique slope for the survival curve (with a D value of 9.5 min) resulted, with a 4 log decrease of the initial bacteria population, always within 40 min of exposure. When PMW has increased to

200 W, the N atom concentration increased to 2.9×10^{21} m^{-3} and the sterile level (–6 log) was reached after 40 min exposure. Again, the survival curve has a unique slope, with a D value of 6.5 min.

Considering these results, the N atom concentration appears to be the key parameter controlling the biocidal efficiency of the Ar–N_2 afterglow, as previously reported by Villeger et al.[7] for the pure N_2 afterglow.

The synergy between the chemical action of the active species of the afterglows and the treatment temperature has already been demonstrated in N_2–O_2 mixtures.[6,23] With the pure nitrogen afterglow, it is also necessary to increase the treatment temperature up to 60°C to reach the sterile level in 40 min (Fig. 11). With the Ar–15%N_2 afterglow, the same biocidal level can be obtained at a temperature much closer to room temperature (T = 32°C). Notably, the survival curves obtained with the pure N_2 afterglow at 60°C and with the Ar–15%N_2 afterglow at 32°C are very similar (unique slope and similar D values), which seems to indicate that the increase of the N atom concentration "compensated" for the heating effect.

V. CONCLUSION

In pure nitrogen, it was previously found that it was necessary to add heating to 60°C to the late afterglow exposure to obtain the sterile state in 40 min in the presence of *E. coli* bacteria. Here, the afterglows of Ar–N_2 mixtures were studied to improve the production of nitrogen atoms. The Ar–15%N_2 mixture produced an increase in N atoms by a factor

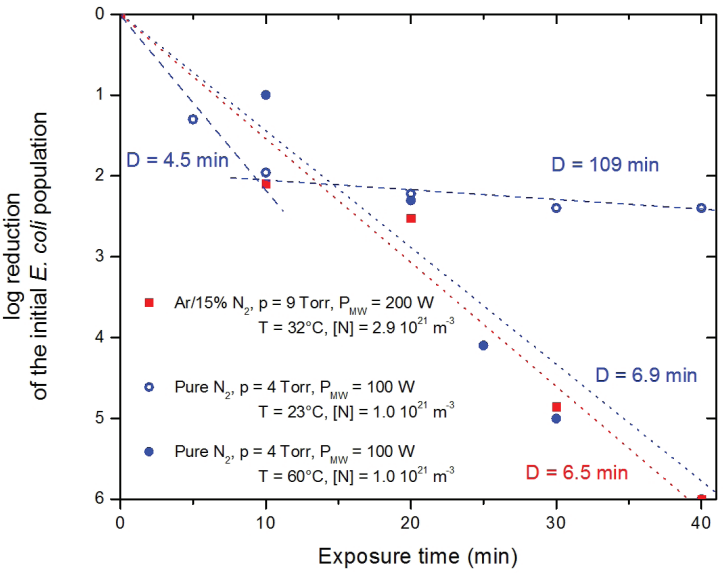

FIG. 11: Effect of temperature on the survival curves of *E. coli* exposed to the pure N_2 late afterglows and comparison with the Ar–15%N_2 afterglow exposure. (d = 5 cm, $Q_{carrier}$ = 1.0 slpm). Linear least-square fits are given, with the corresponding D values.

of two, without substantially modifying the late afterglow conditions or the production of other potentially active species, such as the NO(B) state, responsible for the main UV emission of the afterglow, or the N_2(A) metastable state.

The increase in N concentration made it possible to obtain the sterile level at a temperature of 32°C with the Ar–15%N_2 mixture; therefore, nitrogen is the principal chemical species involved in the death of bacteria. In O_2 containing late afterglows, cell death is supposed to be the consequence of membrane etching by the O atoms and of damage caused to the DNA by UV radiation. As the etching power of the N atoms is low compared with that of the O atoms and the UV production is low in N_2 and Ar–N_2 late afterglows, future work must further investigate the biocidal mechanisms of these afterglows.

ACKNOWLEDGMENTS

This work was supported by the French ANR program PLASMAVIV.

REFERENCES

1. Rossi F, Kylian O, Rauscher H, Hasiwa M, Gilliland D. Low pressure plasma discharges for the sterilization and decontamination of surfaces. New J Phys. 2009;11:115017.
2. Ehlbeck J, Schnabel U, Polak M, Winter J, Von Woedtke T, Brandenburg R, Von Dem Hagen T, Weltmann KD. Low temperature atmospheric pressure plasma sources for microbial decontamination. J Phys D: Appl Phys. 2011;44:013002.
3. Ben Gadri R, Reece Roth J, Montie TC, Kelly-Wintenberg K, Tsai PPY, Helfritch DJ, Feldman P, Sherman DM, Karakaya F, Chen Z, UTK Plasma Sterilization Team. Sterilization and plasma processing of room temperature surfaces with a one atmosphere uniform glow discharge plasma (OAUGDP). Surf Coat Technol. 2000;131:528-542.
4. Halfmann H, Bibinov N, Wunderlich J, Awakowicz P. A double inductively coupled plasma for sterilization of medical devices. J Phys D: Appl Phys. 2007;40:4145-4154.
5. Moisan M, Barbeau J, Moreau S, Pelletier J, Tabrizian M, Yahia L. Low-temperature sterilization using gas plasmas: a review of the experiments and an analysis of the inactivation mechanisms. Int J Pharmaceutics. 2001;226:1-21.
6. Villeger S, Sarrette JP, Ricard A. Synergy between N and O atom action and substrate surface temperature in a sterilization process using a flowing N2-O2 microwave post-discharge. Plasma Process Polym. 2005;2:709-714.
7. Villeger S, Sarrette JP, Rouffet B, Cousty S, Ricard A. Treatment of flat and hollow substrates by a pure nitrogen fowing post-discharge. Eur Phys J Appl Phys. 2008;42:25-32.
8. Krčma F, Žáková M. Pink afterglow in nitrogen-argon mixtures. Eur Phys J D. 2009;54:369-375.
9. Bockel S, Diamy AM, Ricard A. Optical diagnostics of active species in N2 microwave flowing post-discharges. Surf Coat Technol. 1995;74-75:474-478.
10. Boudam MK, Saoudi B, Moisan M, Ricard A. Characterization of the flowing afterglows of an N_2-O_2 reduced-pressure discharge : setting the opering conditions to achieve a dominant late afterglow and correlating the NOβ UV intensity variation with the N and O atom densities. J Phys D: Appl Phys. 2007;40:1694-1711.
11. Loiseau JF, Pignolet P, Held B. Numerical simulation of Ar-N2 excitation transfer in flowing afterglow. J Phys D: Appl Phys. 1992;25:745-750.

12. Piper LG, Cowles LM, Rawlins WT. State to state excitation of NO($A^2\Sigma^+$, v ' = 0,1,2) by $N_2(A^3\Sigma_u^+$, v ' = 0,1,2). J Chem Phys. 1986;85:3369-3378.
13. Brennen W, Gutowski RV, Shane EC. Vibrational distributions of $N_2(A^3\Sigma_u^+)$ in the nitrogen afterglow. Chem Phys Letters. 1974;27:138-140.
14. Dilecce G, De Benedictis S. Experimental studies on elementary kinetics in N_2-O_2 pulsed discharges. Plasma Sources Sci Technol. 1999;8:266-278.
15. Sadeghi N, Foissac C, Supiot P. Kinetics of $N_2(A^3\Sigma_u^+)$ molecules and ionization mechanisms in the afterglow of a flowing N2 microwave discharge. J Phys D: Appl Phys. 2001;34:1779-1788.
16. Shemansky DE. N_2 Vegard-Kaplan system in absorption. J Chem Phys. 1969;51:689-700.
17. Levaton J, Amorim J, Souza AR, Franco D, Ricard A. Kinetics of atoms, metastable, radiative and ionic species in the nitrogen pink afterglow. J Phys D: Appl Phys. 2002;35: 689-699.
18. Pointu AM, Ricard A, Odic E, Ganciu M. Nitrogen atmospheric pressure post discharges for surface biological decontamination inside small diameter tubes. Plasma Process Polym. 2008;5:559-568.
19. Pointu AM, Mintusov E, Fromy P. Study of an atmospheric pressure flowing afterglow in N_2/NO mixture and its application to the measurement of $N_2(A)$ concentration. Plasma Sources Sci Technol. 2010;19:015018.
20. Kossyi IA, Kostinsky AY, Matveyev AA, Silakov VP. Kinetic scheme of the non-equilibrium discharge in nitrogen-oxygen mixtures. Plasma Sources Sci Technol. 1992;1: 207-220.
21. Lerouge S, Fozza AC, Wertheimer MR, Marchand R, Yahia L'H. Sterilization by low-pressure plasma : The role of Vacuum-Ultraviolet radiation. Plasmas and Polymers. 2000; 5:31-46.
22. Lindberg C, Horneck G. Action spectra for survival and spore photoproduct formation of Bacillus subtilis irradiated with short-wavelength (200-300 nm) UV at atmospheric pressure and in vacuo. J Photochem Photobiol B, Biol. 1991;11:69-80.
23. Boudam MK, Moisan M. Synergy effect of heat and UV photons on bacterial-spore inactivation in an N_2-O_2 plasma afterglow sterilizer. J Phys D: Appl Phys. 2010;43:295202.
24. Britun N, Gaillard M, Ricard A, Kim YM, Kim KS, Han JG. Determination of the vibrational, rotational and electron temperatures in N_2 and Ar-N_2 rf discharge. J Phys D: Appl Phys. 2007;40:1022-1029.